Subcritical Growth of Coherent Phase-Space Structures

M. Lesur[1,2] and P. H. Diamond[2,3]

[1]Itoh Research Center for Plasma Turbulence, Kasuga, Kasuga Koen 6-1, 816-8580, Kyushu University, Japan
[2]WCI Center for Fusion Theory, NFRI, Daejeon 305-333, Korea
[3]Center for Momentum Transport and Flow Organization and Center for Astrophysics and Space Sciences, UCSD, La Jolla, CA 92093, USA

Corresponding Author: maxime.lesur@gmail.com

Abstract:

In the presence of wave dissipation, phase-space structures emerge in nonlinear Vlasov dynamics. A new theory gives a simple relation between the growth of these coherent structures and wave energy. The structures can drive the wave by direct momentum exchange, which explains the existence of nonlinear instabilities in both barely unstable and linearly stable (subcritical) regimes. When dissipation is modeled by a linear term in the field equation, simple expressions of a single hole growth rate and of the initial perturbation threshold are in agreement with numerical simulations.

1   Introduction

We consider the fully nonlinear evolution of resonant plasma-wave interactions in the presence of self trapped structures [1]. In this work, we derive a new theory, which shows the relation between wave energy and phase-space density auto-correlation. The mechanisms involved are relevant to many resonance-driven instabilities in laboratory and space plasmas, in particular in the context of energetic particle interaction with Alfvén waves, collisionless trapped electron modes and trapped ion ITG instabilities. To illustrate our theory, we choose two simple models, which treat one-dimensional plasma. The first model is the bump-on-tail instability [2], which is a fundamental paradigm for the basic process of Langmuir waves driven by a supra-thermal population. The Berk-Breizman (BB) extension of the bump-on-tail model includes an external wave damping γ_d to account for linear dissipative mechanisms of the wave energy to the background plasma [3]. The second model is the current-driven ion-acoustic (CDIA) instability, which is a fundamental paradigm for sound-like waves driven by a velocity drift between thermal ions and thermal electrons.

In both models, finite wave damping (externally applied in the BB model; due to ion Landau damping in the CDIA model) allows for the spontaneous creation of self-

trapped structures in the two-dimensional (2D) phase-space, called holes and clumps, whose median velocity evolves in time, resulting in spectral components with a frequency shift $\delta\omega(t)$ (chirping). The growth of phase-space structures results from momentum exchange between particles and wave, or between species, which is due to the dissipation acting on structures. The evolution of holes and clumps is a self-organization process, which provides the energy required to balance dissipation.

For the BB model, in the collisionless, single wave, single structure limit, the growth rate of a structure of size Δv is proportional to $\gamma_d \Delta v \partial_v f_0$. Our simulations confirm the validity of this result in both subcritical and supercritical conditions.

Instabilities in a regime where the wave is linearly stable (subcritical instabilities) have been observed in BB simulations [3, 4] and CDIA simulations [5]. Based on the theory, we explain the mechanism of subcritical instabilities as follows. Landau damping generates a seed phase-space structure, whose growth rate can be positive if the growth due to momentum exchange overcomes the decay due to collisions. In addition, our theory predicts the existence of a nonlinear instability in the marginally unstable regime, which we confirm in our simulations.

2 Models

2.1 Berk-Breizman model

We adopt a perturbative approach, and cast the BB model in a reduced form, which describes the time evolution of the beam particles only [3, 6]. In this sense, we note that the BB model with extrinsic dissipation is also applicable to the traveling wave tube "quasilinear experiment" with a lossy helix [7]. In this model, a single electrostatic wave with a wave number k is assumed and the real frequency of the wave is set to $\omega = \omega_p$, the Langmuir plasma frequency. The evolution of the beam distribution, $f(x, v, t)$, is given by a kinetic equation,

$$\frac{\partial f}{\partial t} + v \frac{\partial f}{\partial x} + \frac{q\tilde{E}}{m} \frac{\partial f}{\partial v} = -\nu_a \delta f + \frac{\nu_f^2}{k} \frac{\partial \delta f}{\partial v} + \frac{\nu_d^3}{k^2} \frac{\partial^2 \delta f}{\partial v^2}, \tag{1}$$

where $\delta f \equiv f - f_0$, $f_0(v)$ is the initial velocity distribution. The evolution of the pseudo-electric field $E \equiv Z \exp i\zeta + c.c.$ is given by

$$\frac{\mathrm{d}Z}{\mathrm{d}t} = -\frac{m\omega_p^3}{4\pi q n_0} \int f(x, v, t) \, e^{-i\zeta} \, \mathrm{d}x \, \mathrm{d}v \, - \, \gamma_d \, Z, \tag{2}$$

where $\zeta \equiv kx - \omega t$, and n_0 is the total density.

We use the COBBLES code [4] to solve the initial-value problem described above. In our simulations, the velocity distribution f_0 is designed with a constant slope between $v = -v_R$ and $v = 3v_R$, where $v_R = \omega/k$ is the resonant velocity. We choose an experimentally-relevant slope with $\gamma_{L0}/\omega = 0.1$ [8], where $\gamma_{L0} = (\pi\omega^3)/(2k^2 n_0)\partial_v f_0$ is a measure of the slope such that $\gamma \sim \gamma_{L0} - \gamma_d$.

2.2   Ion-acoustic model

In this model we evolve two species $s = i, e$ and the electric field self-consistently, assume collisions are negligible, and do not filter a particular wave number. The CDIA model is composed of two kinetic equations,

$$\frac{\partial f_s}{\partial t} + v \frac{\partial f_s}{\partial x} + \frac{q_s E}{m_s} \frac{\partial f_s}{\partial v} = 0, \tag{3}$$

and a current equation,

$$\frac{\partial E}{\partial t} = -\frac{m \omega_p^2}{n_0 q^2} \sum_s \int v f_s(x, v, t) \, \mathrm{d}v. \tag{4}$$

Our code COBBLES can also treat the above model. In our simulations, the initial velocity distributions $f_{0,s}$ are two Gaussians with thermal velocity $v_{th,s}$ centered at $v = v_s$.

3   Energy/Phasestrophy theorem

We can draw a parallel between 2D ideal fluids and 1D Vlasov plasmas. Both are 2D Hamiltonian systems whose evolution is constrained by two invariants: energy and enstrophy in the fluid case, wave energy and phasestrophy in the Vlasov case. This parallel suggests that we can use a common strategy, which is based on solution of the two coupled energy and enstrophy (fluid) or phasestrophy and wave energy (plasma) equations, respectively.

The equations below can be applied to the BB case by removing the subscript s; or to the CDIA case by taking $\gamma_d = \nu_a = \nu_f = \nu_d = 0$. The evolution of phase-space structures is described by the phasestrophy [9, 10],

$$\Psi_s \equiv \int_{-\infty}^{\infty} \left\langle \delta f_s^2 \right\rangle \mathrm{d}v \tag{5}$$

where angle brackets denote the spatial average.

Simple algebra yields an exact relation for the evolution of phasestrophy,

$$\frac{\mathrm{d}\Psi_s}{\mathrm{d}t} = -2 \frac{q_s}{m_s} \int_{-\infty}^{\infty} \frac{\mathrm{d}f_{0,s}}{\mathrm{d}v} \left\langle E \, \delta f_s \right\rangle \mathrm{d}v - \gamma_\Psi^{\mathrm{col}} \Psi_s, \tag{6}$$

where $\gamma_\Psi^{\mathrm{col}}$ is the decay rate of phasestrophy due to collisions,

$$\gamma_\Psi^{\mathrm{col}} = 2\nu_a + \frac{2}{\Psi_s} \frac{\nu_d^3}{k^2} \int_{-\infty}^{\infty} \left\langle \left(\frac{\partial \delta f_s}{\partial v} \right)^2 \right\rangle \mathrm{d}v. \tag{7}$$

The wave energy equation is

$$\frac{\mathrm{d}W}{\mathrm{d}t} + 2\gamma_d W = -2 \sum_s u_s q_s \int \left\langle E \, \delta f_s \right\rangle \mathrm{d}v, \tag{8}$$
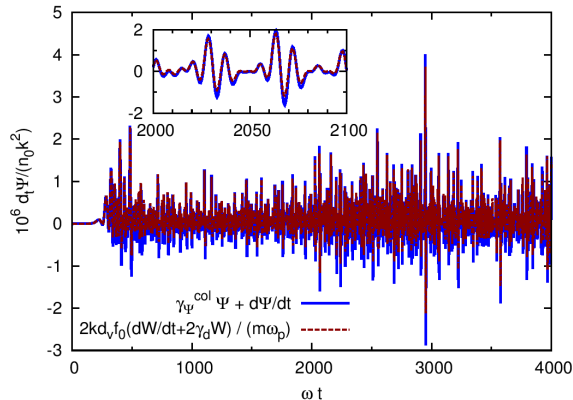
FIG. 1: *Growth of phasestrophy and wave energy in the BB case. Inset: zoom on a smaller timescale. Simulation parameters are $\gamma_{L0}/\omega = 0.1$, $\gamma_d/\gamma_{L0} = 0.7$, $\nu_a/\gamma_{L0} = 10^{-3}$ and $\nu_f = \nu_d = 0$.*
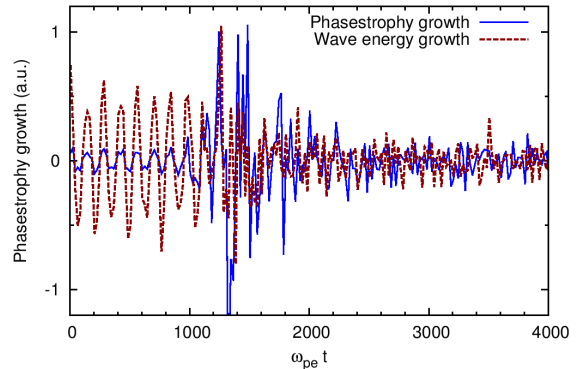
FIG. 2: *Growth of phasestrophy and wave energy in the CDIA case. Parameters are $m_i/m_e = 4$, $v_{th,e}/v_{th,i} = 2$, and $(v_e - v_i)/v_{th,i} = 3$, which is below the linear stability threshold (3.92).*

where $W = n_0 q^2 \langle E^2 \rangle /(m\omega_p^2)$ is the total wave energy, including sloshing energy. In the BB case, $u_s = \omega_p/(2k)$. In the CDIA case, we assumed that the dominant phase-space structures are localized in a neighborhood of $v = u_s$. We assume that $f_{0,s}$ has a constant slope in the velocity-range spanned by evolving phase-space structures, which is satisfied in our simulations (exactly in the BB case; approximately in the CDIA case). Then, phasestrophy evolution is linked to the wave energy evolution, by

$$\frac{\mathrm{d}W}{\mathrm{d}t} + 2\gamma_d W = \sum_s \frac{m_s u_s}{\mathrm{d}_v f_{0,s}} \left(\gamma_\Psi^{\mathrm{col}} + \frac{\mathrm{d}}{\mathrm{d}t} \right) \Psi_s. \tag{9}$$

In parallel with quasi-geostrophic fluids, this relation is the kinetic counterpart of the Charney-Drazin non-acceleration theorem [11]. Fig. 1 shows a good quantitative agreement between the lhs and the rhs in a BB simulation. Fig. 2 shows a qualitative agreement between the lhs and the rhs in a CDIA simulation, where we have substituted u_s by the velocity of maximum overlap between $f_{0,i}$ and $f_{0,e}$, $u_s = 1.42 v_{th,i}$. The disagreement for $\omega_{pe} t < 1000$ corresponds to a phase where structures are not localized around $v = u_s$. Other cases with different parameters show similar levels of agreement (not shown here). Since phasestrophy is directly related to the perturbed momentum in the collisionless limit, $\Psi_s = -2\mathrm{d}_v f_{0,s} \int v \langle \delta f_s \rangle \mathrm{d}v$, phasestrophy growth implies an exchange of momentum, between structures and waves, or between species.

4   Single structure limit

In the BB case, we can apply this theory to calculate the nonlinear growth rate of an isolated structure. We assume that δf is of the form $\delta f = \langle \delta f \rangle [1 + \cos(kx + \theta)]$, with a Gaussian profile, $\langle \delta f \rangle = h(t) \exp[-(v - v_0(t))^2/(2\Delta v(t)^2)]$. This shape corresponds

to a Bernstein-Green-Kruskal mode, which was shown to be a state of maximum entropy subject to constant mass, momentum, and energy [1]. To relate W to Ψ, we use the Poisson equation, even though (in the BB model) it is only approximately satisfied,

$$W = \frac{1}{2}\frac{m\omega_p^2}{k^2 n_0}\left(\int \langle \delta f \rangle \,\mathrm{d}v\right)^2. \tag{10}$$

Thus the evolution of phasestrophy follows a simple expression, $\mathrm{d}\Psi/\mathrm{d}t = \left(\gamma_\Psi - \gamma_\Psi^{\mathrm{col}}\right)\Psi$, where γ_Ψ is the collisionless phase-space structure growth-rate,

$$\gamma_\Psi \approx \frac{16}{3\sqrt{\pi}}\frac{\Delta v}{v_R}\frac{\gamma_{L0}}{\omega_p}\gamma_d. \tag{11}$$

To be concise, in this expression for γ_Ψ we assumed $\Delta v\, d_v f_0 \ll k n_0/\omega$ and $\dot{\Delta v} \ll \gamma_d \Delta v$, which are satisfied in our simulations. Eq. (11) is in qualitative agreement with the collisionless structure growth-rate estimated in Ref. [12]. However, the method used in the reference assumes that $\partial E_0/\partial t \ll \gamma_d E_0$, which is only valid in the initial, linear phase, near marginal stability. Fig. 3 shows the growth of phasestrophy, averaged over a time window of duration $\gamma_{L0}\Delta t = 100$, where Δv in the expression of γ_Ψ is estimated by fitting a Gaussian to $\langle \delta f \rangle$ in the vicinity of the hole at each time-step. We observe a quantitative agreement between our simulations and theory for the supercritical case ($\gamma_d/\gamma_{L0} = 0.5$), and a qualitative agreement in the subcritical case ($\gamma_d/\gamma_{L0} = 1.05$). There is a 40% discrepancy in the subcritical case, which is due in part to the co-existence of a secondary hole with 20% as much phasestrophy as that of the main hole. This suggests that consideration of the primary-secondary hole interaction is necessary to improve the accuracy of the theory.
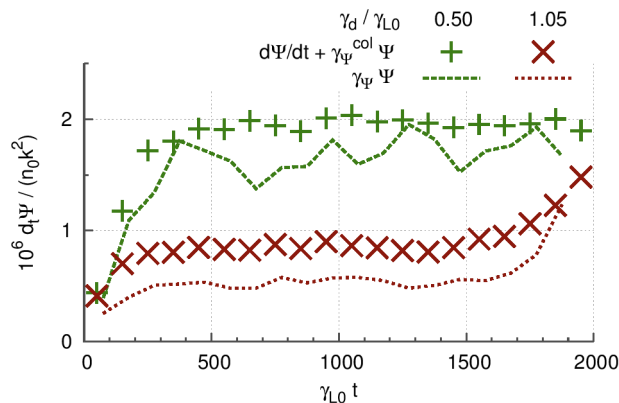
FIG. 3: *Growth rate of the phasestrophy of one isolated hole. Simulation parameters are* $\gamma_{L0}/\omega = 0.1$, $\nu_a = 0$, $\nu_f/\gamma_{L0} = 0.3$, $\nu_d/\gamma_{L0} = 0.17$, *and two different values of* γ_d, *which are given in the legend. Points: phasestrophy growth measured in simulations, including contribution from collisions. Dashed curves: theory, Eq. (11).*
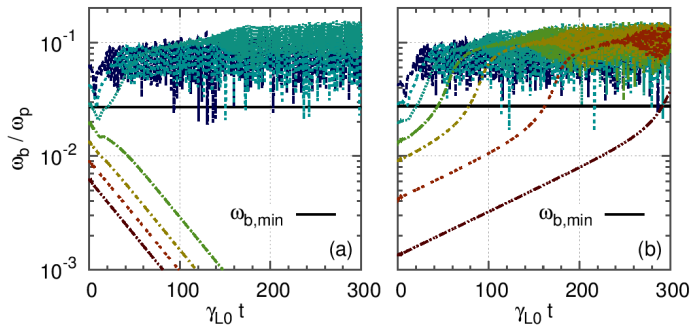
FIG. 4: Dashed curves: time-series of electric field amplitude for different initial amplitudes. (a) Subcritical case, $\gamma_d/\gamma_{L0} = 1.05$. (b) Supercritical case, $\gamma_d/\gamma_{L0} = 0.98$. The other simulation parameters are given in Fig. 3. Solid line: theoretical nonlinear instability threshold, Eq. (12).
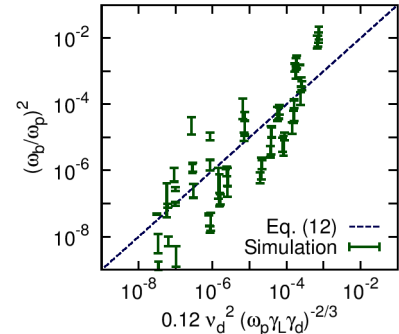
FIG. 5: Nonlinear instability threshold. Vertical bars: range of electric field amplitude between the highest stable and the lowest unstable simulation. Solid line: analytic theory, Eq. (12).

5   Nonlinear instability

Eq. (11) shows that the growth of structures is independent of linear stability, since it is not related to the sign of the total linear growth rate $\gamma \approx \gamma_{L0} - \gamma_d$. Nonlinear growth requires a positive γ_d to enable momentum exchange, a positive slope for f_0 to provide free energy, and a seed structure with a width Δv large enough for γ_Ψ to overcome collisions. When the linear growth rate γ is negative, the seed structure is the hole (clump) corresponding to the $v > v_R$ ($v < v_R$) part of the plateau, which is formed by particles trapped in the finite initial electric field.

The nonlinear instability threshold is obtained by balancing the growth due to dissipation with the decay due to collisions. If Krook-like collisions are negligible, then $\gamma_\Psi^{col} \sim \nu_d^3/(k\Delta v)^2$ and $\Delta v_{min}/v_R \sim 0.7\nu_d(\omega_p\gamma_{L0}\gamma_d)^{-1/3}$. The width of the electrostatic potential well is $4\omega_b/k$, which is twice the width of a seed hole. Here, the electric field amplitude is measured by the bounce-frequency $\omega_b = 2k|qZ|/m$. Thus, the initial amplitude threshold $\omega_{b,min}$ is of the order of

$$\left(\frac{\omega_{b,min}}{\omega_p}\right)^2 \sim 0.12\left(\frac{\omega_p}{\gamma_{L0}}\frac{\omega_p}{\gamma_d}\right)^{2/3}\left(\frac{\nu_d}{\omega_p}\right)^2. \tag{12}$$

Fig. 4(a) shows time-series of electric field amplitude ω_b for different initial amplitudes, for the case $\gamma_d/\gamma_{L0} = 1.05$, which is a subcritical instability with $\gamma/\gamma_{L0} = -0.045$. The threshold between damped solutions and nonlinear instabilities is in agreement with Eq. (12). We further investigate the validity of this scaling by performing a scan of $\gamma_{L0}/\omega_p = 0.02 - 0.50$, $\gamma_d/\gamma_{L0} = 1.01 - 1.20$ and $\nu_d/\gamma_{L0} = 2 \cdot 10^{-3} - 0.1$. For each case, a series of simulation with different initial amplitudes is performed, and we measure, after one island turnover, the amplitude of the highest stable solution and the amplitude of the lowest stable solution. Fig. 5 shows the range of the instability threshold. There is a rough qualitative agreement with our theory. The discrepancy is expected since Eq. (12)

corresponds to a single-hole limit, whereas most cases in Fig. 5 feature two or more dominant holes and clumps. The picture of Landau damping seeding the structure is valid only if the plateau shrinks slowly enough, $|\dot\omega_b| \ll \omega_b^2$. This condition must be satisfied during at least one orbit, which gives an additional condition on the initial amplitude, namely $\omega_b \gg (\pi + 1/2)|\gamma|$. Alternatively put, we don't expect subcritical instabilities when damping exceeds $\gamma_{d,\max} = \gamma_{L0} + 0.3\,\omega_b$.

Subcritical instabilities have also been explained in terms of a nonlinear reduction of ion Landau damping by particle trapping [13]. The mechanism of nonlinear drive we discussed in this paper is different since, in the BB case, external damping is fixed; and in the CDIA case, the nonlinear modification of the ion distribution can not account for the measured growth rates.

In addition, our theory predicts the existence of a nonlinear instability for positive but small γ. For a plateau of width $2\Delta v$, $\Psi \sim \Delta v^3$ and the growth due to the linear instability is $\dot{\Delta v}/\Delta v = \gamma/2$. Then the nonlinear instability due to phasestrophy growth is stronger than the linear growth if $\gamma_\Psi - \gamma_\Psi^{\mathrm{col}} > (3/2)\gamma$. Our simulations confirm for the first time the existence of such supercritical nonlinear instabilities for $0 < \gamma/\gamma_{L0} < 0.04$. Fig. 4(b) shows time-series of electric field amplitude ω_b for different initial amplitudes, for $\gamma_d/\gamma_{L0} = 0.98$, which is slightly above marginal stability with $\gamma/\gamma_{L0} = 0.018$. The threshold where the linear growth becomes nonlinear is in agreement with Eq. (12).

6   Conclusions

We obtain a general relation between wave energy and phasestrophy. This relation can be applied in the BB case to obtain a simple expression for the growth rate of a single phase-space structure, $\gamma_\Psi \sim \gamma_d \gamma_{L0} \Delta v$ in the collisionless limit. This expression shows that dissipation drives a nonlinear instability of holes and clumps via momentum exchange, regardless of linear stability. This leads to faster-than-linear growth in barely unstable regimes, as well as to subcritical instabilities, subject to the presence of a finite seed structure. Simulations in both subcritical and supercritical regimes show a good agreement with analytic theory. The growth rate was obtained in the single structure case. Although we expect similar physical processes in the presence of multiple holes and clumps, the theory should be revisited by taking into account multi-structure interactions. This will likely necessitate some form of turbulence closure theory. The calculation of structure growth rate in the presence of multiple resonances [14] would be the logical next step.

Acknowledgments

References

[1] DUPREE, T. H., "Theory of phase-space density holes", Phys. Fluids 25 (1982) 277.

[2] BERNSTEIN, I. B., TREHAN, S., WEENINK, M., "Plasma Oscillations: II. Kinetic theory of waves in plasmas", Nucl. Fusion 4 (1964) 61.

[3] BERK, H. L., et al., "Spontaneous hole-clump pair creation", Phys. Plasmas 6 (1999) 3102.

[4] LESUR, M., IDOMURA, Y., GARBET, X., "Fully nonlinear features of the energetic beam-driven instability", Phys. Plasmas 16 (2009) 092305.

[5] BERMAN, R. H., et al., "Computer Simulation of Nonlinear Ion-Electron Instability", Phys. Rev. Lett. 48 (1982) 1249.

[6] LESUR, M., IDOMURA, Y., "Nonlinear categorization of the energetic-beam-driven instability with drag and diffusion", Nucl. Fusion 52 (2012) 094004.

[7] TSUNODA, S. I., DOVEIL, F., MALMBERG, J. H., "Nonlinear Interaction between a Warm Electron Beam and a Single Wave", Phys. Rev. Lett. 59 (1987) 2752.

[8] LESUR, M., et al., "Spectroscopic determination of kinetic parameters for frequency sweeping Alfvén eigenmodes", Phys. Plasmas 17 (2010) 122311.

[9] DIAMOND, P., ITOH, S., ITOH, K., Modern Plasma Physics: Volume 1, Physical Kinetics of Turbulent Plasmas, Cambridge University Press (2010).

[10] KOSUGA, Y., DIAMOND, P. H., "On relaxation and transport in gyrokinetic drift wave turbulence with zonal flow", Phys. Plasmas 18 (2011) 122305.

[11] CHARNEY, J. G., DRAZIN, P. G., "Propagation of planetary-scale disturbances from the lower into the upper atmosphere", J. Geophys. Research 66 (1961) 83.

[12] DIAMOND, P. H., KOSUGA, Y., LESUR, M., Dynamics of structures in configuration space and phase space, Festival de Théorie, Aix-en-Provence (2011).

[13] NGUYEN, C., et al., "Existence of metastable kinetic modes", Phys. Rev. Lett. 105 (2010) 205002.

[14] ESCANDE, D. F., ELSKENS, Y., "Microscopic dynamics of plasmas and chaos: the waveparticle interaction paradigm", Plasma Phys. Control. Fusion 45 (2003) A115.